RSC Advances

PAPER

View Article Online
View Journal | View Issue

Cite this: *RSC Adv.*, 2015, **5**, 46608

Benzimidazolium-based chemosensors: selective recognition of $H_2PO_4^-$, $HP_2O_7^{3-}$, F^- and ATP through fluorescence and gelation studies†

Kumaresh Ghosh,*[a] Debasis Kar,[a] Debashis Sahu[b] and Bishwajit Ganguly*[b]

Received 9th April 2015
Accepted 22nd April 2015

DOI: 10.1039/c5ra06301a

www.rsc.org/advances

Benzimidazolium-based receptors **1** and **2** have been designed and synthesized. The receptors with identical binding sites exhibit different sensing properties towards different anions under identical conditions. In a lower equivalent amount of guests, receptors **1** and **2** show fluorescence selectivity towards phosphate-based anions. In the presence of higher equivalent amounts of guests, while structure **1** reveals selectivity in sensing of phosphate derivatives such as hydrogen pyrophosphate and dihydrogenphosphate in CH_3CN, under identical conditions receptor structure **2** senses F^-. Furthermore, compounds **1** and **2** validate the visual sensing of hydrogen pyrophosphate and dihydrogenphosphate, respectively, through the formation of gels. Binding studies have been carried out using fluorescence, UV-vis, ^1H NMR and ^{31}P NMR spectroscopic techniques. Experimental results have been correlated with the theoretical findings.

Introduction

The design and synthesis of artificial fluorescent receptors for the selective sensing of anionic substrates is of immense interest in the field of supramolecular research.[1] Anions play crucial roles in a wide range of chemical and biological processes.[2] Inorganic phosphates or phosphate-based biomolecules are considered to be important due to their involvement in many biochemical reactions.[3] Of the different inorganic phosphates, hydrogen pyrophosphate or pyrophosphate (PPi) draws attention because not only it is the product of ATP hydrolysis under cellular conditions but also is involved in DNA sequencing/replication, *etc.* In addition to being a structural component in bones and teeth, it plays roles in energy storage and signal transduction.[4]

Fluoride, on the other hand, draws attention because of its severe role in environmental and biological systems. Fluoride is linked with dental and skeletal fluorosis.[5] Fluoride is accused of causing osteosarcoma[6] and of exerting some effect at the brain level. Inhibition of neurotransmitter biosynthesis in foetuses caused by a high concentration of fluoride is also documented.[7] Alarm is raised by the fact that fluoride is introduced in the environment by many anthropogenic activities, especially in relation to the use of phosphate-containing fertilizers and aluminium processing industries. Thus, given the importance of these anions, their selective sensing is desirable and much effort has been directed for their recognition in the last few years.[1,4,8]

Of the different types of receptor structures, the fluorescent-based compounds have much potential due to high sensitivity and detection feasibility. In this regard, the design and synthesis of a fluorescent receptor which shows recognition of multiple anions with a subtle variation in structure is of keen interest in anion recognition. A recent report from our group shows that replacement of butyryl amide by 1-naphthyl acetamide in pyridinium motif-based tripodal receptors introduces recognition of different nucleotides.[9a] Similarly, a pyridinium motif-based isophthaloyl diamide binding site with different appended fluorophores has been observed to detect and sense different anions with moderate to good selectivities.[9b,c] Caltagirone *et al.* reported some bis-ureidic receptors that show variation in anion sensing when phenyl urea is replaced by naphthyl urea.[9d] Moreover, a subtle variation in the binding site in an anthracene-based ditopic receptor enabled us to recognise fluorometrically the different aliphatic dicarboxylates.[9e]

[a]*Department of Chemistry, University of Kalyani, Kalyani-741235, India. E-mail: ghosh_k2003@yahoo.co.in; Fax: +913325828282; Tel: +913325828750*

[b]*Computation and Simulation Unit, Analytical Discipline and Centralized Instrument Facility, Academy of Scientific and Innovative Research CSIR-Central Salt and Marine Chemicals Research Institute, Bhavnagar, Gujarat, 364002, India. E-mail: ganguly@csmcri.org*

† Electronic supplementary information (ESI) available: Figures showing the change in fluorescence and absorbance of receptors **1** and **2** with different Job plots, binding curves, a table for the gelation study and pictures, DFT structures, ^1H and ^{13}C NMR and mass spectra, and Cartesian coordinates of all the optimized geometries along with their absolute energies. See DOI: 10.1039/c5ra06301a

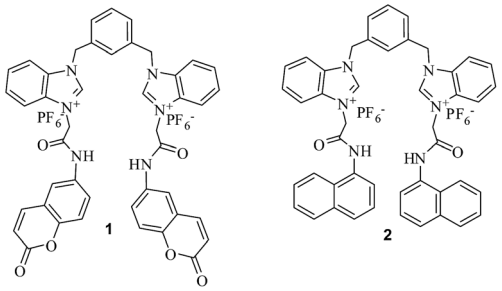

Along this direction, we now report here two easily made new structures, **1** and **2**, which possess identical binding sites with different fluorogenic units and exhibit different anion sensing behaviours. While structure **1** reveals selectivity in sensing of phosphate derivatives such as hydrogen pyrophosphate and dihydrogenphosphate in CH_3CN, under identical conditions structure **2** shows a preference for F^-.

Results and discussion

The chemosensors **1** and **2** were synthesized according to Scheme 1. The benzimidazole groups were first coupled with 1,3-dibromomethylbenzene to afford compound **3**[10a,b] which on reflux with different chloroamides **4** and **5** in dry CH_3CN for 1 day produced the dichloride salts **1a** and **2a**, respectively. Anion exchange of the dichloride salts using NH_4PF_6 in aqueous CH_3OH afforded the desired compounds **1** and **2** in appreciable yields. All the compounds were characterised by usual spectroscopic techniques.

The molecular recognition properties of the benzimidazolium salts **1** and **2** were evaluated by UV-vis, fluorescence and ^1H NMR spectroscopic methods. The fluorescence spectrum of **1** in CH_3CN gave a broad band at 430 nm when excited at 340 nm. The change in emission of **1** ($c = 3.16 \times 10^{-5}$ M) in the presence of 15 equiv. amounts of different anionic guests (taken as their tetrabutylammonium salts) was observed to be different and the results are accumulated in Fig. 1a. As can be seen from Fig. 1a, structure **1** has a strong propensity for phosphate-based anions. Among the different phosphates, hydrogen pyrophosphate ($HP_2O_7^{3-}$) and dihydrogenphosphate ($H_2PO_4^-$) strongly perturbed the emission of **1**. In the presence of 2 equiv. amounts of

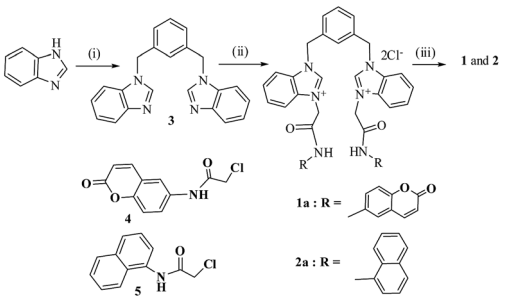

Scheme 1 Reagents and conditions: (i) NaH, 1,3-dibromomethylbenzene, dry THF, reflux, 6 h; (ii) $RNHCOCH_2Cl$, CH_3CN and a few drops of DMF, reflux, 1 day; (iii) NH_4PF_6, aqueous CH_3OH, stirred for 1/2 h.

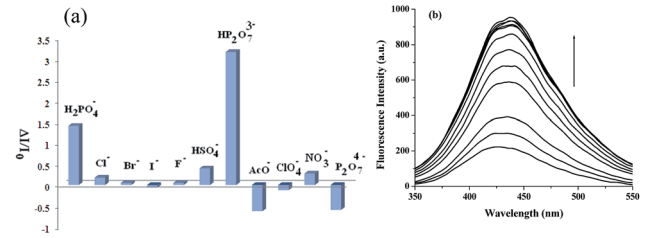

Fig. 1 (a) Change in the fluorescence ratio of **1** ($c = 3.16 \times 10^{-5}$ M) at 430 nm upon addition of 15 equiv. amounts of different anions (counter ions: tetrabutylammonium cations) in CH_3CN; (b) change in the emission of **1** ($c = 3.16 \times 10^{-5}$ M) upon addition of $(Bu_4N)_3HP_2O_7$ ($c = 1 \times 10^{-3}$ M).

$H_2PO_4^-$, the change in the emission of **1** was greater compared to the case of 15 equiv. amounts of the anion (Fig. 3S†). However, pyrophosphate ($P_2O_7^{4-}$) weakly changed the emission of **1** in the opposite mode to $HP_2O_7^{3-}$. This has relevance in the distinction of $P_2O_7^{4-}$ from $HP_2O_7^{3-}$. The emission titration spectrum of **1** with $HP_2O_7^{3-}$ is depicted in Fig. 1b.

On moving from receptor **1** to **2**, which provides an identical binding site with different fluorophores, a different selectivity in fluorescence for the same set of anions was observed under identical conditions. In the presence of 2 equiv. amounts of anions, receptor **2** shows a preference for $H_2PO_4^-$ (ESI, Fig. 6S†). This may be due to the orientation of naphthalene motifs in **2** which possibly regulates the size of the pseudo cavity. Interestingly, when higher equivalent amounts of anions were individually added to the receptor solution of **2**, a fluorescence selectivity for the F^- ion was observed. In the presence of higher equivalent amounts of $H_2PO_4^-$, the emission intensity of **2** started to decrease (ESI, Fig. 6S†). This may occur due to decomplexation of $H_2PO_4^-$ or conversion of bound $H_2PO_4^-$ into PO_4^{3-}.[11a] Fig. 2 displays the change in the fluorescence ratio of **2** ($c = 3.27 \times 10^{-5}$ M) in CH_3CN at a longer wavelength (~510 nm) in the presence of 15 equiv. amounts of different anions. In the series, only the most basic anion F^- brought about a significant change in emission. Fig. 3a represents the titration spectra for **2** with F^-. The selective enhancement of emission at the longer wavelength of 510 nm in the presence of F^- is likely to be due to a chelation-induced excimer between the naphthalene motifs in **2**. The excitation spectra of the complex of **2** with F^- were collected at the monomer (370 nm) and excimer emission (510

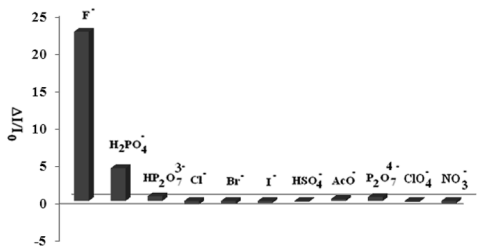

Fig. 2 Change in the fluorescence ratio of **2** ($c = 3.27 \times 10^{-5}$ M) at 510 nm upon addition of 15 equiv. amounts of different anions (counter ions: tetrabutylammonium cations) in CH_3CN.

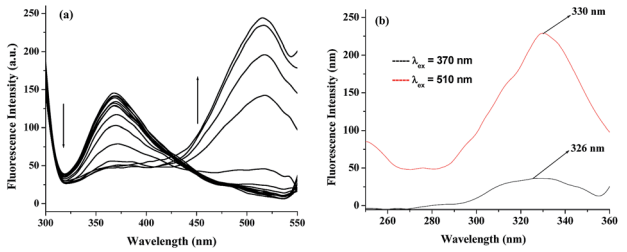

Fig. 3 (a) Change in emission of **2** ($c = 3.27 \times 10^{-5}$ M) upon addition of F^- ($c = 1 \times 10^{-3}$ M); (b) excitation spectra of the complex of **2** with 15 equiv. amounts of Bu_4NF (collected at the monomer and excimer emission maxima).

nm) maxima. The excitation spectrum of the excimer emission was observed to be positionally unchanged with the excitation spectrum of the monomer emission (Fig. 3b). This revealed the formation of the dynamic excimer rather than the static excimer.[10c]

The ground state interaction of the receptors **1** and **2** with all the anions was understood by conducting UV-vis titration experiments. In most cases, irregular and small changes suggested a weak interaction (ESI†). Both **1** and **2** formed 1 : 1 complexes[11b] with $HP_2O_7^{3-}$ and F^-, respectively (ESI, Fig. 7S†). Binding constants were determined using the emission titration data[12a] in CH_3CN (ESI, Fig. 8S†). The receptor **1** binds dihydrogenphosphate and hydrogen pyrophosphate with binding constant (K_a) values of 3.67×10^3 M^{-1} and 4.10×10^4 M^{-1}, respectively. The detection limit[12b] (ESI†) for hydrogen pyrophosphate is determined to be 2.59×10^{-6} M. On the other hand, receptor **2** binds F^- with a K_a of 4.11×10^3 M^{-1} and the detection limit is observed to be 1.81×10^{-4} M. Due to the minor change in emission, it was difficult to determine K_a for other anions.

The selectivity in the binding process was understood by observing the emission behaviour of the receptors upon addition of a particular anionic substrate to the solution of a receptor containing other interfering anions. In this context, Fig. 4A shows the selectivity of **1** for $HP_2O_7^{3-}$. It is evident from Fig. 4A that only $H_2PO_4^-$ ions moderately interfered in the binding of the $HP_2O_7^{3-}$ ion. Similarly, Fig. 4B demonstrates the selectivity profile for **2** with F^- where only $H_2PO_4^-$ ions interfered negligibly.

To investigate the binding features of the receptors in an aqueous system, emission titrations with different phosphate salts as well as phosphate group-containing biomolecules such as ATP, ADP and AMP were carried out in aq. CH_3CN ($CH_3CN : H_2O = 1 : 1$, v/v, pH = 7.3 using 10 mM HEPES buffer). Due to insolubility of the receptors either with PF_6^- or Cl^- counterions in pure water, aqueous CH_3CN was used as a compromised solvent system. However, in this solvent system, the change in emission of **1** was found to be marginally greater in the presence of tetrabutylammonium hydrogen pyrophosphate (ESI, Fig. 11S†) and the stoichiometry of the complex[11b] was determined as 1 : 1 (Fig. 12S†) with a binding constant[12a] of 9.1×10^3 M^{-1} (Fig. 13S†). During complexation of $HP_2O_7^{3-}$ into the cleft, the intensity of the peak at 434 nm was gradually decreased (ESI, Fig. 11S†). A similar study with the same guests was performed with receptor **2** (ESI, Fig. 14S†). Among the guests taken, ATP brought a greater change in emission in aq. CH_3CN ($CH_3CN : H_2O = 1 : 1$, v/v, pH = 7.3 using 10 mM HEPES buffer). Fig. 5A demonstrates the change in the fluorescence ratio of **2** ($c = 3.06 \times 10^{-5}$ M) at 400 nm upon addition of 15 equiv. amounts of different phosphate-containing guests and fluoride in aq. CH_3CN ($CH_3CN : H_2O = 1 : 1$ v/v, pH = 7.3 using 10 mM HEPES buffer) and Fig. 5B represents the fluorescence titration spectra of **2** with ATP. The binding constant value for **2** with ATP was determined to be 2.85×10^3 M^{-1} (ESI, Fig. 15S†).

It is noted that the fluorescence titrations of **1** and **2** with the same anions including the S^{2-} ion in aq. CH_3CN ($CH_3CN : H_2O = 1 : 1$, v/v) without using a buffer introduced a similar trend as that observed at pH 7.3 (ESI, Fig. 16S†).

In order to identify the interacting protons of **1** in the binding of $HP_2O_7^{3-}$, $P_2O_7^{4-}$ and $H_2PO_4^-$, we recorded ^1H NMR of **1** in the presence of 1 equiv. amount of $HP_2O_7^{3-}$ (Fig. 6A), $P_2O_7^{4-}$ (Fig. 18S†) in d_6-DMSO and $H_2PO_4^-$ in $CDCl_3$ containing 10% d_6-DMSO (Fig. 6B). The use of different NMR solvents was undertaken in the study based on the consideration of the solubility of receptors in NMR concentration range in the presence of guests. However, as can be seen from Fig. 6, upon

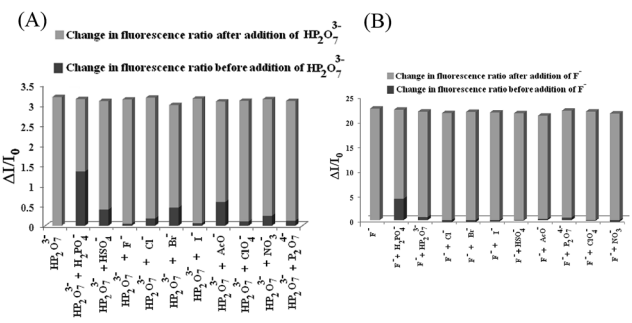

Fig. 4 Change in fluorescence ratios of (A) **1** ($c = 3.28 \times 10^{-5}$ M) upon addition of 15 equiv. amounts of $HP_2O_7^{3-}$ in the presence and absence of other anions in CH_3CN; (B) **2** ($c = 3.20 \times 10^{-5}$ M) upon addition of 15 equiv. amounts of F^- in the presence and absence of other anions in CH_3CN (counter cations of salts: tetrabutylammonium ions).

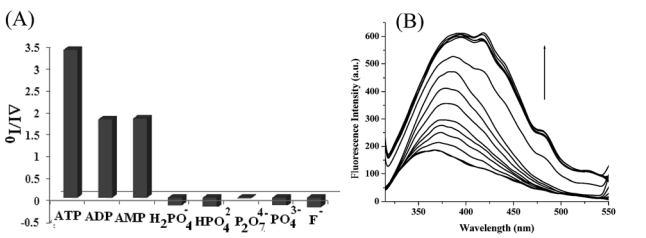

Fig. 5 (A) Change in the fluorescence ratio of **2** ($c = 3.06 \times 10^{-5}$ M) at 400 nm upon addition of 15 equiv. amounts of different phosphate-containing anions (counter cation: sodium ion) and potassium fluoride in $CH_3CN : H_2O$ (1 : 1 v/v, pH = 7.3 using 10 mM HEPES buffer); (B) change in emission of **2** ($c = 3.06 \times 10^{-5}$ M) upon addition of 15 equiv. amounts of ATP ($c = 1 \times 10^{-5}$ M) in $CH_3CN : H_2O$ (1 : 1 v/v, pH = 7.3 using 10 mM HEPES buffer).

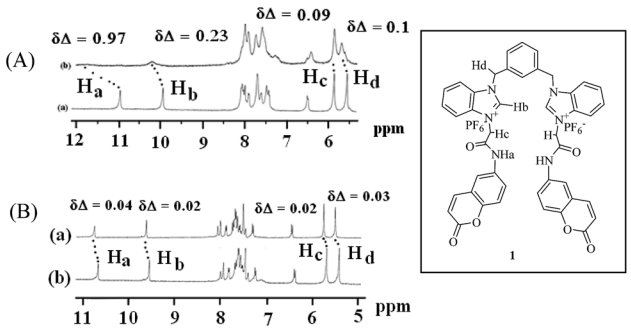

Fig. 6 (A) Partial ^{1}H NMR spectra (400 MHz) of **1** ($c = 4.26 \times 10^{-3}$ M) in the absence (a) and presence of an equivalent amount of $(Bu_4N)_3HP_2O_7$ (b) in d_6-DMSO; (B) partial ^{1}H NMR spectra (400 MHz) of **1** ($c = 3.28 \times 10^{-3}$ M) in the presence (a) and absence of an equivalent amount of $(Bu_4N)H_2PO_4$ (b) in $CDCl_3$ containing 10% d_6-DMSO.

complexation of $HP_2O_7^{3-}$ the signals for amide protons (H_a) and benzimidazolium protons (H_b) of **1** moved to the downfield direction by 0.97 ppm and 0.23 ppm, respectively. Aromatic protons showed a weak upfield chemical shift and the signals for –CH_2– groups (H_d) underwent a minor downfield chemical shift (0.1 ppm). In comparison, addition of an equivalent amount of $(Bu_4N)_4P_2O_7$ to the solution of **1** in d_6-DMSO brought about an almost insignificant change in the chemical shift values of both the amide and benzimidazolium protons (ESI, Fig. 17S†) and thereby suggested its negligible interaction with the receptor. When $H_2PO_4^-$ was added to the solution of **1** in $CDCl_3$ containing 10% d_6-DMSO (Fig. 6B), amide protons (H_a) and benzimidazolium protons (H_b) showed downfield chemical shifts of 0.04 ppm and 0.02 ppm, respectively, and indicated a moderate interaction like $HP_2O_7^{3-}$. During interaction the signals for the aromatic ring protons also indicated a small downfield shift.

Similarly, we recorded ^{1}H NMR of **2** in the presence of F^- (Fig. 7) in $CDCl_3$ containing 10% d_6-DMSO. Upon gradual addition of F^-, the amide proton moved to the downfield direction and became broad. In the presence of 15 equiv. amounts of F^-, the amide protons appeared at 11.87 ppm as a broad peak and thereby the possibility of formation of HF_2^- through deprotonation was ignored. The signals for benzimidazolium protons (H_b) and methylene protons of types H_c and H_d exhibited a downfield movement (Fig. 7). The naphthalene ring proton (H_e) also exhibited a downfield shift.

Thus the observations from ^{1}H NMR for both **1** and **2** corroborate that the anions are complexed into the cavities of the receptors involving mostly the benzimidazolium (H_b) and amide (H_a) protons. Participation of the methylene protons of types H_c and H_d in the interaction with the anions, although weak in nature, can not be ignored.

In addition to ^{1}H NMR, a ^{31}P NMR study was also performed for **1** and **2** in the presence of selective phosphate-based anions. Receptor **1** perturbed the P-signals of $HP_2O_7^{3-}$ by showing a change in the chemical shift values. The signals for the different P-atoms in $HP_2O_7^{3-}$ merged upon complexation with **1** (Fig. 8A). In the case of $H_2PO_4^-$, the signal of the P-atom suffered a downfield chemical shift by 0.15 ppm in the presence of 1 equiv. amount of **1** in d_6-DMSO (Fig. 8B). The P-atom in $H_2PO_4^-$ in the presence of **2** moved downfield weakly by 0.06 ppm (Fig. 9). Such findings on either upfield or downfield chemical shifts of the signals for P-atoms of different phosphates support their interaction into the pseudo cavities of the receptors due to which the P-atoms suffer small shielding and deshielding effects.

In a semi-aqueous system, we also recorded ^{31}P NMR of the guests in the presence of the receptors. In d_6-DMSO : D_2O (1 : 1, v/v), the α and β phosphorus atoms of $HP_2O_7^{3-}$ appeared at −1.23 ppm and −7.11 ppm, respectively. In the presence of **1**, α-phosphorus showed an upfield chemical shift of 1.74 ppm (ESI, Fig. 18S†). The signal for α-phosphorus was not found and we presume that this becomes equivalent to β-phosphorus on deprotonation. Similarly, the α, β and γ P-atoms in ATP underwent a small chemical shift change in the presence of **2**. The γ-P was shifted by 0.13 ppm and suggested its weak participation in complexation with **2** (ESI, Fig. 19S†). This is in accordance with the moderate change in emission of **2** during titration with ATP (Fig. 5B).

Interestingly, during binding studies of the receptors in organic solvents, the gelation behaviours of **1** and **2** in the presence of some selected anions were observed. This further extended the scope of these structures in the visual recognition of anions. Compound **1** (taken in 10 mg mL^{-1}) formed a gel instantly in DMSO in the presence of 1 equiv. amount of $(Bu_4N)_3HP_2O_7$ (Fig. 20S†). Other anions in the study failed to do so. This unique feature distinguished $HP_2O_7^{3-}$ from the other anions examined.

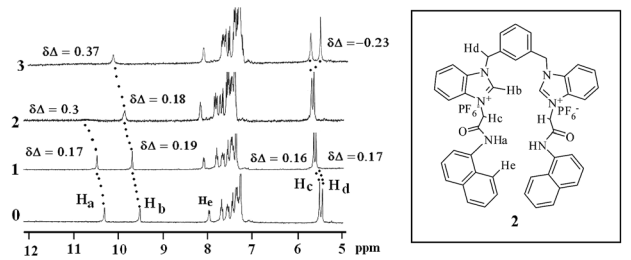

Fig. 7 ^{1}H NMR ($CDCl_3$ containing 10% d_6-DMSO, 400 MHz) titration using receptor **2** ($c = 4.08 \times 10^{-3}$ M) and Bu_4NF (numbers in the margin designate the number of equivalents added).

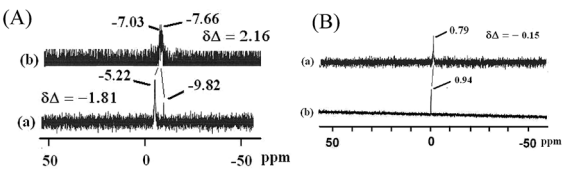

Fig. 8 (A) ^{31}P NMR spectra of (a) $(Bu_4N)_3HP_2O_7$ ($c = 3.18 \times 10^{-3}$ M) and (b) with an equiv. amount of receptor **1** ($c = 3.18 \times 10^{-3}$ M) in d_6-DMSO; (B) ^{31}P NMR spectra of (a) $(Bu_4N)H_2PO_4$ ($c = 4.28 \times 10^{-3}$ M) and (b) with an equiv. amount of receptor **1** ($c = 4.28 \times 10^{-3}$ M) in d_6-DMSO.

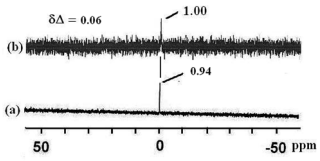

Fig. 9 ^{31}P NMR spectra of (a) $(Bu_4N)H_2PO_4$ ($c = 4.35 \times 10^{-3}$ M) and (b) with an equiv. amount of receptor **2** ($c = 4.35 \times 10^{-3}$ M) in d_6-DMSO.

It is noted that in spite of a small change in fluorescence of **2** in the presence of 15 equiv. amounts of $H_2PO_4^-$ (Fig. 2), receptor **2** formed a brown-colored gel with a minimum gelation concentration of 10 mg mL^{-1} upon addition of 1 equiv. amount of $(Bu_4N)H_2PO_4$ in DMSO. This describes the strong interaction of receptor **2** with $H_2PO_4^-$. This is in accordance with the greater change in fluorescence (Fig. 6S†) of **2** in the presence of 2 equiv. amounts of $H_2PO_4^-$. However, the other anions did not show any gelation property with **2**. Solvent variations with different dielectric constants were examined for the gelation study (Table 1S†). From SEM images, the fibrous and granular three-dimensional architectures were noted for **1** and **2**, respectively (Fig. 10). We believe that guest-induced intermolecular chelation of the benzimidazolium-based receptors gives some supramolecular network in the solution due to which solvent molecules are entrapped and gelation takes place. In this aspect, the recognition of $(Bu_4N)H_2PO_4$ and $(Bu_4N)_3HP_2O_7$ through gelation using synthetic receptors is rarely known in the literature.[8n]

Computational study

To understand the binding structures as well as the reason behind the diversity of the receptor structures in anion recognition, we performed DFT calculations on the receptors **1** and **2** (Fig. 11) with various anions in a CH_3CN medium. In the case of **1**, a stronger fluorescence intensity of receptor **1** is observed with $HP_2O_7^{3-}$ and then $H_2PO_4^-$ compared to the other anions in both lower (2 equiv.; ESI†) as well as higher concentrations (15 equiv.) of the guest anions at 430 nm experimentally. To understand such anion recognition, we have calculated the binding energies of $HP_2O_7^{3-}$ and $H_2PO_4^-$ with receptor **1** at the B3LYP-D1/6-31G(d)//B3LYP/6-31G(d) level of theory. The calculated results show that the binding energy of receptor **1** with $HP_2O_7^{3-}$ (−72.3 kcal mol^{-1}) is much higher than that of

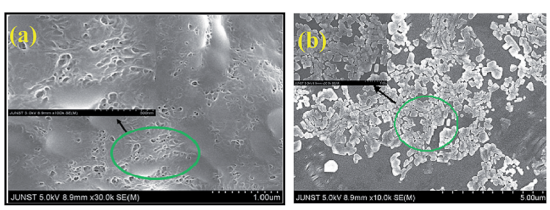

Fig. 10 SEM images of xero gels of (a) **1** with 1 equiv. amount of $(Bu_4N)_3HP_2O_7$ and (b) **2** with 1 equiv. amount of $(Bu_4N)H_2PO_4$ from DMSO.

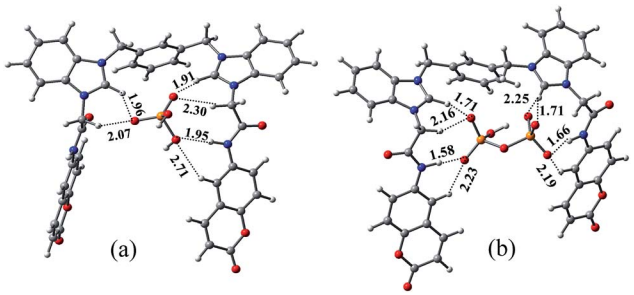

Fig. 11 The H-bonding distances between the fluorophore units of **1** with the guests (a) $H_2PO_4^-$ and (b) $HP_2O_7^{3-}$. All the distances are given in Å.

$H_2PO_4^-$ (−36.3 kcal mol^{-1}). The stronger binding of $HP_2O_7^{3-}$ is due to the greater number of interactions with the fluorophore units of **1** than $H_2PO_4^-$ (Fig. 11). Again, the energy gap between the highest occupied molecular orbital (HOMO) and the lowest unoccupied molecular orbital (LUMO) ($\Delta E_{LUMO-HOMO}$) of the complex between receptor **1** and $HP_2O_7^{3-}$ is lower (2.6 eV) than that of the complex between receptor **1** and $H_2PO_4^-$ (3.5 eV).

Therefore, the charge transfer[13–15] between the fluorophore units of receptor **1** in the presence of $HP_2O_7^{3-}$ can easily be the possible explanation for strong fluorescence intensity in this case (Fig. 12). In the optimized structure of receptor **1** with the pyrophosphate ($P_2O_7^{4-}$), it was observed that one of the oxygen atoms of pyrorophosphate abstracts the proton from one amide nitrogen atom of **1** while the other oxygen atom of $P_2O_7^{4-}$ makes a covalent bond to the benzimidazolium carbon atom. This abnormality of the $P_2O_7^{4-}$ anion may seem to be responsible for the quenching of the fluorescence for receptor **1** compared to the hydrogen pyrophosphate ($HP_2O_7^{3-}$) case (Fig. 22S†).

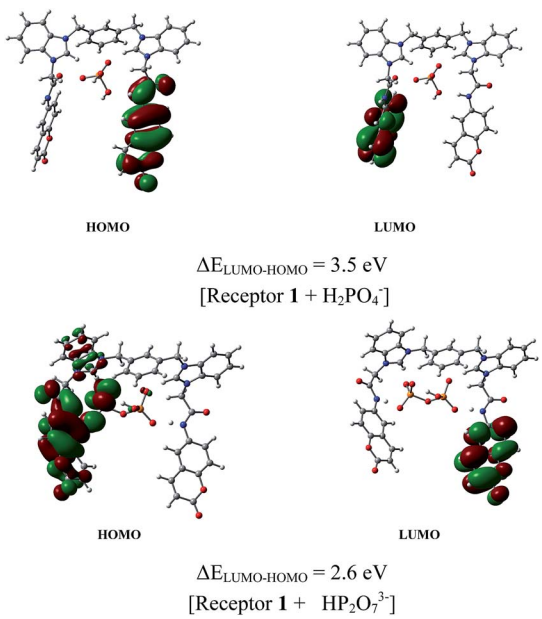

Fig. 12 Frontier molecular orbitals of the B3LYP/6-31G(d) optimized complexes of receptor **1** with $H_2PO_4^-$ and $HP_2O_7^{3-}$.

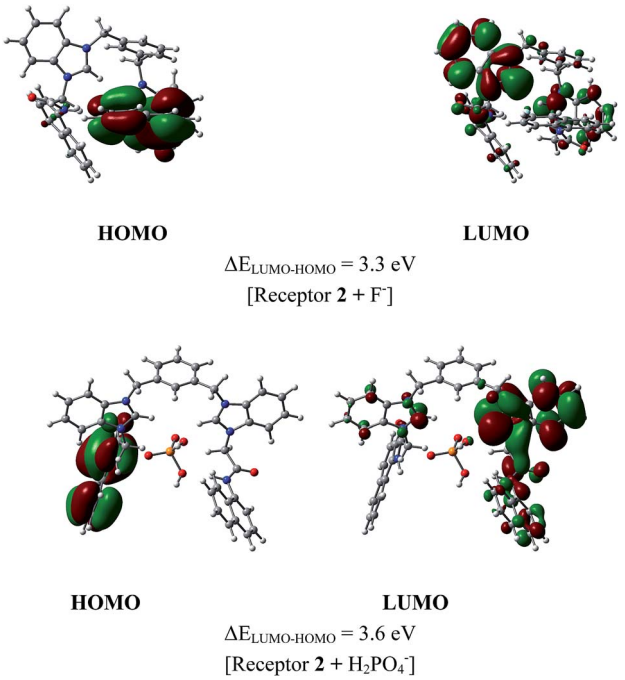

Fig. 13 Frontier molecular orbitals of the B3LYP/6-31G(d) optimized complexes of receptor **2** with F^- and $H_2PO_4^-$.

However, in the case of receptor **2**, strong fluorescence intensities are observed with $H_2PO_4^-$ and then $HP_2O_7^{3-}$ at the lower concentration (2 equiv.) of the anionic guests, while at a higher concentration (15 equiv.) of the guests, strong fluorescence intensities are observed with F^- and then $H_2PO_4^-$ at 510 nm experimentally. The B3LYP-D1/6-31G(d)//B3LYP/6-31G(d) calculated binding energies show that F^- is more strongly complexed (-94.6 kcal mol^{-1}) to receptor **2** than $H_2PO_4^-$ (-39.3 kcal mol^{-1}) in a CH_3CN medium. The HOMO–LUMO energy gap ($\Delta E_{LUMO-HOMO}$) in the complex between receptor **2** and F^- (3.3 eV) is also lower than that in the complex with $H_2PO_4^-$ (3.6 eV). Therefore, charge transfer from one fluorophore unit to another unit is favourable in the complex of F^- with **2** to generate strong fluorescence intensity (Fig. 13).

Further, a comparative study using the DFT model shows that the binding energies of F^- with both the receptors are similar in nature but the gap between the HOMO and LUMO for receptor **1** is relatively higher (3.5 eV) (Fig. 23S†) than the gap between the HOMO and LUMO of receptor **2** (3.3 eV). For this reason, receptor **1** presumably shows a smaller change in fluorescence compared to receptor **2**.

Conclusion

The chemosensors **1** and **2** show successful fluorometric recognition of anions such as F^-, $H_2PO_4^-$ and $HP_2O_7^{3-}$ under different conditions involving hydrogen bonding and charge–charge interactions in CH_3CN. In the presence of lower equivalent amounts of anionic guests, while receptor **1** shows fluorescence selectivity towards $HP_2O_7^{3-}$, receptor **2**, with identical binding sites, exhibits a preference for $H_2PO_4^-$. This difference in selectivity for receptors **1** and **2** is presumably attributed to the different dispositions of the appended fluorophores that regulate the dimension of the pseudo cavities where binding takes place. In the presence of higher equivalent amounts of guests, the selectivity profile of **1** remains the same. But receptor **2** shows a preference for the F^- ion. We believe that a strong chelation of the F^- ion involving amide and benzimidazolium protons in the cavity of **2** brings a greater change in fluorescence.

Receptor structures **1** and **2** also validate the visual sensing of hydrogen pyrophosphate and dihydrogenphosphate, respectively, through the formation of supramolecular gels. It is mentionable that the recognition of $H_2PO_4^-$ and $HP_2O_7^{3-}$ through gelation using molecular receptors[8n] is rarely reported in the literature. Thus the present systems in this report are undoubtedly to be the new addendum to the literature.

In aqueous CH_3CN, sensor **2** shows a moderate selectivity towards ATP over ADP and AMP while compound **1** does not exhibit any selectivity. A similar study with our previously reported receptor[10b] with a different fluorophore that exhibited selectivity for other different anions further substantiated the relevance of tuning of the structure that controls their different recognition behaviours. The cavity dimension of the receptors due to different dispositions of the fluorophores around the binding sites, and also sometimes the involvement of ring protons of the fluorophores in complexation of anions, brings such differences in selectivity. DFT calculations with FMO analysis reveal the difference in the fluorescence intensity of receptors with different anions.

Experimental

General procedure of fluorescence and UV-vis titrations

Stock solutions of the receptors were prepared in the selected solvents and 2 mL or 2.5 mL of the individual receptor solution was taken in the cuvette for recording absorption and emission spectra. Stock solutions of anions were prepared in the same solvents, and were individually added in different amounts to the receptor solution and the change in emission and absorbance of the receptors were noted.

Method for Job plot[11b]

The stoichiometry was determined by the continuous variation method (Job plot). In this method, solutions of host and guests of equal concentrations were prepared in the required dry solvents. Then the host and guest solutions were mixed in different proportions maintaining a total volume of 3 mL of the mixture. The related compositions for host : guest (v/v) were 3 : 0, 2.8 : 0.2, 2.5 : 0.5, 2.2 : 0.8, 2 : 1, 1.8 : 1.2, 1.5 : 1.5, 1 : 2, 0.8 : 2.2, 0.5 : 2.5 and 0.2 : 2.8. All the prepared solutions were kept for 1 h with occasional shaking at room temperature. Then emission and absorbance of the solutions of different compositions were recorded. The concentration of the complex, *i.e.* [HG], was calculated using the equation $[HG] = \Delta I/I_0 \times [H]$ or $[HG] = \Delta A/A_0 \times [H]$ where $\Delta I/I_0$ and $\Delta A/A_0$ indicate the relative emission and absorbance intensities. [H] corresponds to the

concentration of the pure host. The mole fraction of the host (X_H) was plotted against concentration of the complex [HG]. In the plot, the mole fraction of the host at which the concentration of the host–guest complex [HG] is maximum gives the stoichiometry of the complex.

Computational details

Full geometrical optimizations were carried out in the gas phase employing the Becke three-parameter hybrid density functional combined with the Lee–Yang–Parr correlation functional (B3LYP)[16–19] with the standard 6-31G(d) basis set.[20] Frequency calculations were performed at the same level of theory to confirm that each stationary point was a local minimum (with zero imaginary frequencies). Single point calculations were executed at the same level of theory, considering the first order dispersion correction (dft-D)[21,22] with a polarizable continuum model (PCM)[23,24] in the CH_3CN medium ($\varepsilon = 36.64$) employing the B3LYP/6-31G(d)-optimized geometries. All DFT calculations were performed with the Gaussian 09 suite of programs.[25]

Synthesis of 1,3-bis((1*H*-benzo[*d*]imdazol-1-yl)methyl) benzene 3.[10a] To a stirred solution of benzimidazole (0.6 g, 5.08 mmol) in dry THF (20 mL), NaH (0.122 g, 5.08 mmol) was added at room temperature. The solution was then refluxed for 1 h. After cooling, 1,3-bisbromomethyl benzene (0.67 g, 2.54 mmol) was added to the reaction mixture. The reaction mixture was further refluxed for 5 h. After completion of the reaction, the THF solvent was removed and water was added to the crude mass. The reaction mixture was then extracted with chloroform containing 2% methanol (50 mL × 3). The combined extracts were dried over Na_2SO_4. Removal of the solvent *in vacuo* and subsequent flash column chromatography (ethyl acetate : petroleum ether 80 : 20, v/v) afforded compound **3** (0.6 g, yield: 69%) as a white crystalline solid: mp 118 °C; ^{1}H NMR (400 MHz, d_6-DMSO) δ 8.37 (2H, s), 7.66 (2H, d, $J = 8$ Hz), 7.43 (2H, m), 7.26 (1H, t, $J = 8$ Hz), 7.19–7.15 (7H, m), 5.46 (4H, s) ppm; ^{13}C NMR (100 MHz, d_6-DMSO) δ 144.1, 143.5, 137.3, 133.5, 129.1, 126.9, 126.8, 122.3, 121.6, 119.4, 110.6, 47.5 ppm; FT-IR: ν in cm^{-1} (KBr): 3246, 3088, 1612, 1496, 1440.

Synthesis of 2-chloro-*N*-(2-oxo-2*H*-chromen-6-yl)acetamide 4. To a stirred solution of 6-aminocoumarin (1 g, 6.21 mmol) in dry CH_2Cl_2 (30 mL), chloroacetyl chloride (0.742 mL, 9.31 mmol) and dry Et_3N (1 mL, 6.83 mmol) were added. The reaction mixture was stirred for 6 h and the progress of the reaction was monitored by TLC. After completion of the reaction, the solvent was removed and the residue was extracted with $CHCl_3$ containing 1% CH_3OH (50 mL × 3). The organic layer was separated, dried over Na_2SO_4 and concentrated under vacuum. The crude residue was purified by column chromatography (eluent: ethyl acetate : petroleum ether, 1 : 1, v/v) to give 2-chloro-*N*-(2-oxo-2*H*-chromen-6-yl) acetamide **4** (1.3 g, 88.16%): mp 178 °C; ^{1}H NMR (400 MHz, $CDCl_3$) δ 8.35 (1H, s), 7.99 (1H, d, $J = 4$ Hz), 7.72 (1H, d, $J = 12$ Hz), 7.52 (1H, dd, $J_1 = 8$ Hz, $J_2 = 4$ Hz), 7.34 (1H, d, $J = 8$ Hz) 6.48 (1H, d, $J = 12$ Hz), 4.23 (2H, s) ppm; FT-IR: ν in cm^{-1} (KBr): 3295, 3102, 1702, 1619, 1573, 1434.

Synthesis of 2-chloro-*N*-(naphthalen-1-yl)acetamide 5. To a stirred solution of naphthalen-1-amine (0.8 g, 5.59 mmol) in dry CH_2Cl_2 (20 mL), chloroacetyl chloride (0.667 mL, 8.38 mmol) and dry Et_3N (0.794 mL, 6.15 mmol) were added. The reaction mixture was then stirred for 7 h. After completion of the reaction, the solvent was removed and the residue was extracted with $CHCl_3$ containing 2% CH_3OH (50 mL × 3). The organic layer was separated, dried over Na_2SO_4 and concentrated under vacuum. The residue was purified by column chromatography (eluent: ethyl acetate : petroleum ether, 1 : 4, v/v) to give 2-chloro-*N*-(naphthalen-1-yl)acetamide **5** (1.0 g, 81.5%): mp 154 °C; ^{1}H NMR (400 MHz, $CDCl_3$) δ 8.78 (1H, s), 7.99 (1H, d, $J = 8$ Hz), 7.89 (2H, t, $J = 8$ Hz), 7.76 (1H, d, $J = 8$ Hz), 7.60–7.49 (3H, m), 4.36 (2H, s) ppm; ^{13}C NMR (100 MHz, $CDCl_3$) δ 164.4, 134.0, 131.1, 128.8, 127.0, 126.6, 126.5, 126.2, 125.6, 120.7, 120.3, 43.3 ppm; FT-IR: ν in cm^{-1} (KBr): 3256, 3052, 1665, 1556, 1505, 1349.

Synthesis of receptor 1. To a stirred solution of compound **3** (0.2 g, 0.591 mmol) in CH_3CN (20 mL) containing a few drops of DMF, 2-chloro-*N*-(2-oxo-2*H*-chromen-6-yl)acetamide **4** (0.308 g, 1.30 mmol) was added and the reaction mixture was refluxed for 48 h. The precipitate that appeared in the reaction mixture was filtered off and washed with hot CH_3CN and ether successively. Finally, the dichloride salt of **1a** was dried under vacuum (0.30 g, 62.4%). To a methanolic solution (15 mL) of the dichloride salt of **1a** (0.1 g, 0.122 mmol), NH_4PF_6 (0.06 g, 0.368 mmol) was added and the solution was stirred for 30 min under warming conditions. After reducing the reaction volume, a small amount of water was added to give a white precipitate. The precipitate was filtered, washed with ether and finally dried under vacuum to afford the pure compound **1** (0.12 g, 94.5%): mp 168 °C; ^{1}H NMR (400 MHz, $CDCl_3$ containing two drops of d_6-DMSO) δ 10.93 (2H, s), 9.92 (2H, s), 8.07 (2H, m), 7.90 (2H, d, $J = 8$ Hz), 7.70–7.59 (8H, m), 7.47 (6H, m), 6.50 (2H, d, $J = 8$ Hz), 5.88 (4H, s), 5.58 (4H, s) ppm; ^{13}C NMR (100 MHz, d_6-DMSO) δ 164.1, 160.3, 150.2, 144.5, 144.2, 135.2, 135.0, 132.5, 130.7, 130.4, 128.9, 128.6, 127.4, 127.1, 123.7, 119.3, 118.4, 117.4, 117.2, 114.5, 114.2, 50.2, 49.6 ppm; FT-IR: ν in cm^{-1} (KBr): 3402, 3109, 1708, 1622, 1567, 1490, 1440; HRMS (EI) calc. for $C_{44}H_{34}F_6N_6O_6P$: 887.2176 $(M - PF_6)^+$; found: 887.2258 $(M - PF_6)^+$.

Synthesis of receptor 2. Compound **2** was prepared according to the experimental procedure as followed for the synthesis of compound **1**. In the reaction, the amounts taken for compounds **3** and **5** were 0.15 g (0.443 mmol) and 0.214 g (0.975 mmol), respectively. After work up, the dichloride salt of **2a** was obtained in a 58.2% yield (0.20 g). To a methanolic solution of the dichloride salt (0.1 g, 0.128 mmol), NH_4PF_6 (0.063 g, 0.385 mmol) was added and the reaction mixture was stirred under warming conditions for 30 min. After reducing the volume of the reaction mixture, a small amount of water was added. A brown precipitate appeared, which was filtered, washed with ether and dried under a high vacuum pump to afford the pure compound **2** (0.12 g, yield: 93.6%): mp 199 °C; ^{1}H NMR (400 MHz, d_6-DMSO) δ 10.65 (2H, s), 9.98 (2H, s), 8.24 (2H, d, $J = 8$ Hz), 8.12 (2H, d, $J = 8$ Hz), 7.98 (2H, d, $J = 8$ Hz), 7.88 (2H, d, $J = 8$ Hz), 7.82 (2H, d, $J = 8$ Hz), 7.74–7.67 (6H, m), 7.63–7.57 (6H, m), 7.53–7.46 (4H, m), 5.87 (4H, s), 5.75 (4H, s) ppm; ^{13}C NMR (100 MHz, d_6-DMSO) δ 164.9, 144.2, 135.2, 134.2, 132.9, 132.4, 130.8, 130.4, 128.9, 128.7, 128.0, 127.4, 127.2, 126.7, 126.5,

126.4, 126.0, 123.1, 122.7, 122.1, 114.4, 114.2, 50.2, 49.5 ppm; FT-IR: ν in cm^{-1} (KBr): 3586, 3388, 3157, 1693, 1567, 1505, 1436; mass (EI): 851.5 $(M - PF_6)^+$, 723.6, 705.6, 522.3; anal calc. $C_{46}H_{38}N_6O_2(PF_6)_2$: C, 55.43; H, 3.84; N, 8.43; found: C, 55.48; H, 3.86; N, 8.47%.

Acknowledgements

We gratefully acknowledge UGC, New Delhi, India for providing facilities in the department under the SAP program. DK thanks CSIR, New Delhi, India for a fellowship.

References

1 (*a*) R. Martinez-Manez and F. Sancenon, *Chem. Rev.*, 2003, **103**, 4419; (*b*) C. Caltagirone and P. A. Gale, *Chem. Soc. Rev.*, 2009, **38**, 520; (*c*) P. A. Gale, S. E. García-Garrido and J. Garric, *Chem. Soc. Rev.*, 2008, **37**, 151; (*d*) Z. Xu, N. J. Singh, J. Lim, J. Pan, H. N. Kim, S. Park, K. S. Kim and J. Yoon, *J. Am. Chem. Soc.*, 2009, **131**, 15528; (*e*) Y. Zhou, Z. Xu and J. Yoon, *Chem. Soc. Rev.*, 2011, **40**, 2222; (*f*) Z. Xu, N. J. Singh, S. K. Kim, D. R. Spring, K. S. Kim and J. Yoon, *Chem.–Eur. J.*, 2011, **17**, 1163; (*g*) Z. Xu, S. K. Kim and J. Yoon, *Chem. Soc. Rev.*, 2010, **39**, 1457; (*h*) M. Wenzel, J. R. Hiscock and P. A. Gale, *Chem. Soc. Rev.*, 2012, **41**, 480; (*i*) M. Wenzel, J. R. Hiscock and P. A. Gale, *Chem. Soc. Rev.*, 2012, **41**, 480; (*j*) N. Ahmed, B. Sirinfar, S. Youn, M. Yousuf and K. S. Kim, *Org. Biomol. Chem.*, 2013, **11**, 6407.

2 (*a*) *Ullman's encyclopedia of industrial chemistry*, Wiley-VCH, New York, NY, Germany, 6th edn, 1998; (*b*) K. L. Krik, *Biochemistry of halogens and inorganic halides*, Plenum, New York, NY, 1991, p. 591; (*c*) K. Rurack and U. Resch-Genger, *Chem. Soc. Rev.*, 2002, **31**, 116; (*d*) J. L. Sessler, P. A. Gale and W. S. Cho, *Anion Receptor Chemistry*, The Royal Society of Chemistry, Cambridge, UK, 2006.

3 (*a*) C. P. Mathews and K. E. van Hold, *Biochemistry*, The Benjamin/Cummings Publishing Company, Inc., Redwood City, CA, 1990; (*b*) S. Xu, M. He, H. Yu, X. Cai, X. Tan, B. Lu and B. Shu, *Anal. Biochem.*, 2001, **299**, 188.

4 A. E. Hargrove, S. Nieto, T. Zhang, J. L. Sessler and E. V. Anslyn, *Chem. Rev.*, 2011, **111**, 6603.

5 S. Ayoob and A. K. Gupta, *Crit. Rev. Environ. Sci. Technol.*, 2006, **36**, 433.

6 E. B. Bassin, D. Wypij and R. B. Davis, *Cancer, Causes Control*, 2006, **17**, 421.

7 Y. Yu, W. Yang, Z. Dong, C. Wan, J. Zhang, J. Liu, K. Xiao, Y. Huang and B. Lu, *Fluoride*, 2008, **41**, 134.

8 (*a*) V. K. Khatri, S. Upreti and P. S. Pandey, *J. Org. Chem.*, 2007, **72**, 10224; (*b*) K. Ghosh and D. Kar, *Beilstein J. Org. Chem.*, 2011, **7**, 254; (*c*) T. Gunnlaugsson, A. P. Davis, J. E. O'Brien and M. Glynn, *Org. Lett.*, 2002, **4**, 2449; (*d*) H. Ihm, S. Yun, H. G. Kim, J. K. Kim and K. S. Kim, *Org. Lett.*, 2002, **4**, 2897; (*e*) K. Choi and A. D. Hamilton, *Angew. Chem., Int. Ed.*, 2001, **40**, 3912; (*f*) C. Caltagirone, A. Mulas, F. Isaia, V. Lippolis, P. A. Gale and M. E. Light, *Chem. Commun.*, 2009, 6279; (*g*) Q. Y. Cao, T. Pradhan, S. Kim and J. S. Kim, *Org. Lett.*, 2011, **13**, 4386; (*h*) S. I. Konodo, Y. Hiraoka, N. Kurumatani and Y. Yano, *Chem. Commun.*, 2005, 1720; (*i*) X. H. Huang, Y. B. He, C. G. Hu and Z. H. Chen, *Eur. J. Org. Chem.*, 2009, 1549; (*j*) H. N. Lee, N. J. Singh, S. K. Kim, J. Y. Kwon, Y. Y. Kim, K. S. Kim and J. Yoon, *Tetrahedron Lett.*, 2007, **48**, 169; (*k*) K. Ghosh, A. R. Sarkar, A. Ghorai and U. Ghosh, *New J. Chem.*, 2012, **36**, 1231; (*l*) K. Ghosh, A. R. Sarkar, A. Sommader and A. R. Khuda-Bukhsh, *Org. Lett.*, 2012, **14**, 4314; (*m*) K. Ghosh, D. Kar, S. Joardar, D. Sahu and B. Ganguly, *RSC Adv.*, 2013, **3**, 16144; (*n*) K. Ghosh, A. R. Sarkar and A. P. Chattopadhyay, *Eur. J. Org. Chem.*, 2012, 1311; (*o*) K. Ghosh, D. Kar, S. Joardar, A. Sommader and A. R. Khuda-Bukhsh, *RSC Adv.*, 2014, **4**, 11590; (*p*) E. J. Songa, H. Kima, I. H. Hwanga, K. B. Kima, A. R. Kimb, I. Nohb and C. Kima, *Sens. Actuators, B*, 2014, **195**, 36; (*q*) J. J. Lee, G. J. Park, Y. W. Choi, G. R. You, Y. S. Kim, S. Y. Lee and C. Kim, *Sens. Actuators, B*, 2015, **207**, 123; (*r*) G. J. Park, H. Y. Jo, K. Y. Ryu and C. Kim, *RSC Adv.*, 2014, **4**, 63882.

9 (*a*) K. Ghosh, D. Tarafdar, A. Sommader and A. R. Khuda-Bukhsh, *RSC Adv.*, 2015, **5**, 35175; (*b*) K. Ghosh and A. R. Sarkar, *Org. Biomol. Chem.*, 2011, **9**, 6551; (*c*) K. Ghosh, A. R. Sarkar and G. Masanta, *Tetrahedron Lett.*, 2007, **48**, 8725; (*d*) C. Caltagirone, C. Bazzicalupi, F. Isaia, M. E. Light, V. Lippolis, R. Montis, S. Murgia, M. Olivari and G. Picci, *Org. Biomol. Chem.*, 2013, **11**, 2445; (*e*) K. Ghosh and G. Masanta, *Tetrahedron Lett.*, 2008, **49**, 2592.

10 (*a*) K. Ghosh, D. Kar, A. Panja, I. D. Petsalakis and G. Theodorakopoulos, *Supramol. Chem.*, 2014, **26**, 856; (*b*) K. Ghosh, D. Kar and P. Ray Chowdhury, *Tetrahedron Lett.*, 2011, **52**, 5098; (*c*) P. K. Lekha, T. Ghosh and E. Prasad, *J. Chem. Sci.*, 2011, **123**, 919.

11 (*a*) P. A. Gale, J. R. Hiscock, S. J. Moore, C. Caltagirone, M. B. Hursthouse and M. E. Light, *Chem.–Asian J.*, 2010, **5**, 555; (*b*) P. Job, *Ann. Chim.*, 1928, **9**, 113.

12 (*a*) P. T. Chou, G. R. Wu, C. Y. Wei, C. C. Cheng, C. P. Chang and F. T. Hung, *J. Phys. Chem. B*, 2000, **104**, 7818; (*b*) A. Caballero, R. Martinez, V. Lioveras, I. Ratera, J. Vidal-Gancedo, K. Wurst, A. Tarraga, P. Molina and J. Vaciana, *J. Am. Chem. Soc.*, 2005, **107**, 1875.

13 H. Sun, D. Zhang, C. Ma and C. Liu, *Int. J. Quantum Chem.*, 2007, **107**, 1875–1885.

14 I. D. Petsalakis, N. N. Lathiotakis and G. Theodorakopoulos, *J. Mol. Struct.: THEOCHEM*, 2008, **867**, 64–70.

15 J. Lim, T. A. Albright, B. R. Martin and O. Š. Miljanić, *J. Org. Chem.*, 2011, **76**, 10207–10219.

16 A. D. Becke, *J. Chem. Phys.*, 1993, **98**, 5648–5652.

17 C. Lee, W. Yang and R. G. Parr, *Phys. Rev. B: Condens. Matter Mater. Phys.*, 1988, **37**, 785–789.

18 B. Miehlich, A. Savin, H. Stoll and H. Preuss, *Chem. Phys. Lett.*, 1989, **157**, 200–206.

19 P. J. Stephens, F. J. Devlin, C. F. Chabalowski and M. J. Frisch, *J. Phys. Chem.*, 1994, **98**, 11623–11627.

20 M. M. Francl, *J. Chem. Phys.*, 1982, **77**, 3654–3665.

21 S. Grimme, J. Antony, S. Ehrlich and H. Krieg, *J. Chem. Phys.*, 2010, **132**, 154104.

22 S. Grimme, *J. Comput. Chem.*, 2004, **25**, 1463–1473.

23 B. Mennucci, J. Tomasi, R. Cammi, J. R. Cheeseman, M. J. Frisch, F. J. Devlin, S. Gabriel and P. J. Stephens, *J. Phys. Chem. A*, 2002, **106**, 6102–6113.

24 M. Cossi, V. Barone, R. Cammi and J. Tomasi, *Chem. Phys. Lett.*, 1996, **255**, 327–335.

25 M. J. Frisch, G. W. Trucks, H. B. Schlegel, G. E. Scuseria, M. A. Robb, J. R. Cheeseman, G. Scalmani, V. Barone, B. Mennucci, G. A. Petersson, H. Nakatsuji, M. Caricato, X. Li, H. P. Hratchian, A. F. Izmaylov, J. Bloino, G. Zheng, J. L. Sonnenberg, M. Hada, M. Ehara, K. Toyota, R. Fukuda, J. Hasegawa, M. Ishida, T. Nakajima, Y. Honda, O. Kitao, H. Nakai, T. Vreven, J. A. Montgomery Jr, J. E. Peralta, F. Ogliaro, M. Bearpark, J. J. Heyd, E. Brothers, K. N. Kudin, V. N. Staroverov, T. Keith, R. Kobayashi, J. Normand, K. Raghavachari, A. Rendell, J. C. Burant, S. S. Iyengar, J. Tomasi, M. Cossi, N. Rega, J. M. Millam, M. Klene, J. E. Knox, J. B. Cross, V. Bakken, C. Adamo, J. Jaramillo, R. Gomperts, R. E. Stratmann, O. Yazyev, A. J. Austin, R. Cammi, C. Pomelli, J. W. Ochterski, R. L. Martin, K. Morokuma, V. G. Zakrzewski, G. A. Voth, P. Salvador, J. J. Dannenberg, S. Dapprich, A. D. Daniels, O. Farkas, J. B. Foresman, J. V. Ortiz, J. Cioslowski, and D. J. Fox, *Gaussian 09, Revis. B01*, Gaussian, Inc., Wallingford, CT, 2010.